Geophysical Signatures of the Keurusselkä Meteorite Impact Structure – Implications for Crater Dimensions

S. Raiskila[1], J. Plado[2], H. Ruotsalainen[3] and L.J. Pesonen[1]*

[1] Department of Physics, University of Helsinki, P.O. Box 64, FIN-00014 Helsinki, Finland
[2] Department of Geology, University of Tartu, Ravila 14a 50411, Estonia
[3] Finnish Geodetic Institute, P.O. Box 15, FIN-02431 Masala, Finland

[*]Corresponding author, e-mail: selen.raiskila@helsinki.fi

Abstract

Terrestrial impact structures carry the effects of shock and impact-related processes on target rocks and minerals. Integration of petrophysical data obtained from surface and drill core rocks with geophysical field studies allows the crater dimensions to be delineated, even when the impact structure is deeply eroded. Our study concentrates on the Mesoproterozoic Keurusselkä impact structure, with paleomagnetic and geochemical ($^{40}Ar/^{39}Ar$) ages of 1120 and 1140 Ma, respectively; and, especially, its central uplift region, which is characterized by the presence of well-defined in-situ shatter cones. The structure is located within the 1900–1860 Ma old granitic Svecofennian domain in central Finland and is deeply eroded. Prominent high-amplitude low-wavelength magnetic anomalies occupy the central uplift region of the structure and are attributed to magnetization caused by a meteorite impact. Corresponding negative gravity anomalies are less distinctive, but are consistent with the magnetic ones. In this paper we present the potential field maps and a geophysical model for the Keurusselkä impact structure. Crater dimensions are are estimated from theoretical equations combined with the modeling results. We propose that the original rim-to-rim diameter of Keurusselkä structure has been 24–27 km.

1   Introduction

The Keurusselkä structure in Finland (62°08'N, 24°37'E, Fig. 1) represents the eroded remain of a complex impact crater (*Raiskila et al.,* 2011*; Dypvik et al.,* 2008). The structure was recognized from in-situ and boulder shatter cones along the shorelines of lake Keurusselkä in 2003 (*Hietala and Moilanen,* 2004*;* 2007) (Fig. 2). *Ferriére et al.* (2010) demonstrated petrographic evidence of shock metamorphic features in quartz (PDFs) that have been formed at pressures up to 20 GPa, thus, confirming the impact origin for Keurusselkä. The PDFs were found from in-situ rocks with shatter cones, located in the central uplift area of the structure. Clearly recognizable shatter cones were found only in metavolcanic/metagranitic rocks (Figs. 1 and 2) (*Raiskila et al.,* 2011). Other more coarse-grained rock types (granite, granodiorite and gneisses) show striated
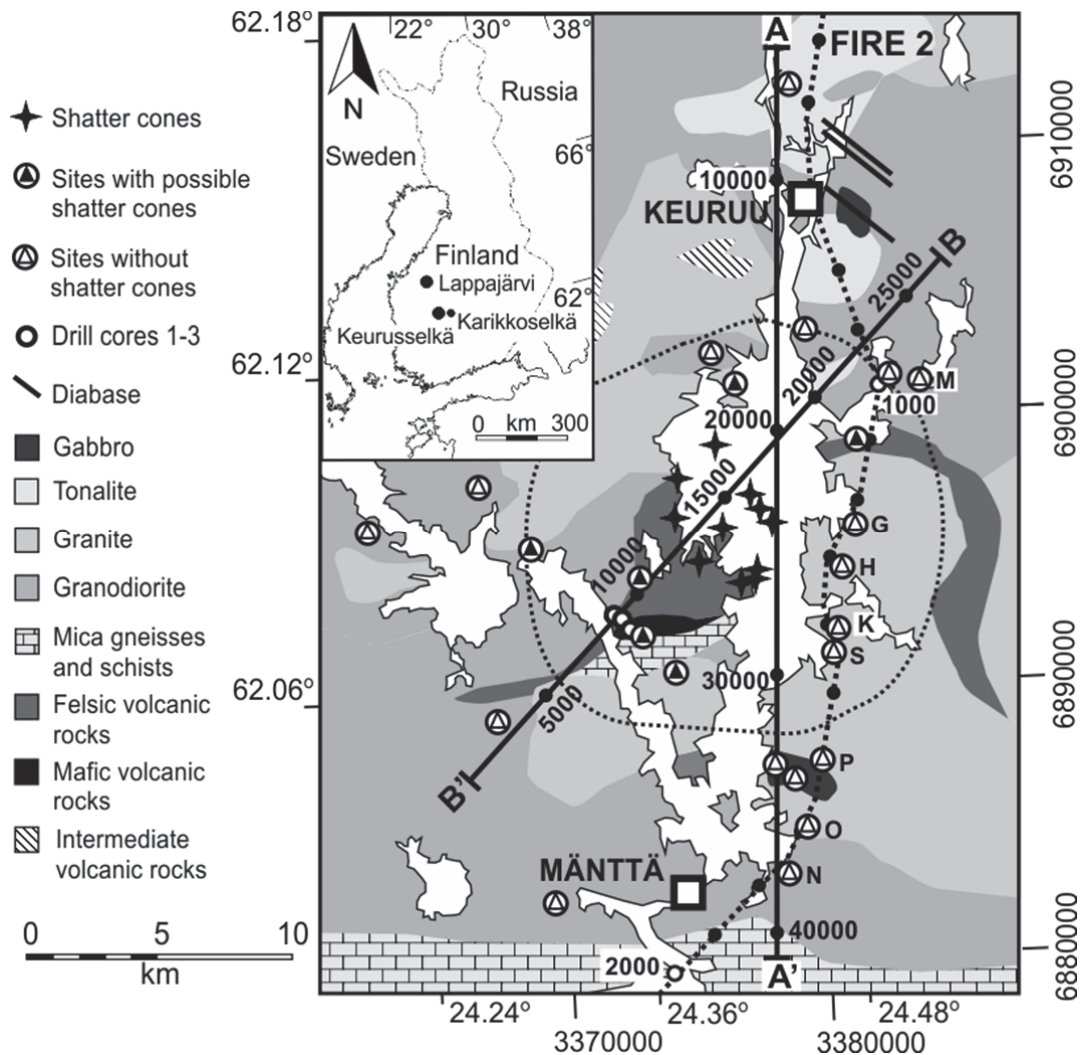
Fig. 1 The geological setting (modified from *Nironen*, 2003) of the study area with sampling sites, two marked profiles (A-A' and B-B') and the FIRE 2 seismic reflection profile. Dotted circular area (D ~ 16 km) marks the boundary of damaged bedrock with low density. The inset shows the location of the Keurusselkä meteorite impact structure together with two nearby locating impact structures, Lappajärvi (D ~23 km, age ~73 Ma) and Karikkoselkä (D ~1.5 km, age ≤ 230 Ma) (modified from *Dypvik et al.*, 2008).

surfaces, which may represent shatter cones without pointing apexes (*Wieland et al.,* 2006; *Baratoux and Melosh,* 2003). *Raiskila et al.* (2011) measured the shatter cone ori-entations, which were noticed to be random rather than pointing to the shock wave cen-ter. We note that the shatter cone formation on impact craters has not yet been solved in a way that explains the exact timing of their formation in a cratering process. However, shatter cones form in the interactions of elastic waves, which explain the variety of shat-ter cone shapes and the range of striation geometries and angles (*Wieland et al.,* 2006). *Raiskila et al.* (2011) introduced the paleomagnetic age estimate (~1120 Ma) for the Keurusselkä structure obtained from shatter cone carrying rocks. It is almost consistent with the $^{40}Ar/^{39}Ar$ dating by *Schmieder et al.* (2009) from a pseudotachylitic breccia vein, located in the boundary between volcanic rock and granitoids on the west side of

the Keurusselkä shoreline (Fig. 1), indicating an age of 1140 ± 6 Ma for the event. However, thin section analysis of this vein showed only planar formations (PFs) (*Schmieder et al.,* 2009), which are not considered as impact features (*French and Koeberl,* 2010) and can be of tectonic origin.

In this study, we present magnetic, gravity and seismic signatures of the Keurusselkä impact structure. A forward two-dimensional model, applying the measured petrophysical properties of rocks, is then introduced to interpret the observed geophysical anomalies. Based on the theoretical crater dimension scaling laws, combined with the magnetic and gravity anomalies and model, we estimate the original crater diameter and the depth of the transient crater of the Keurusselkä impact structure.
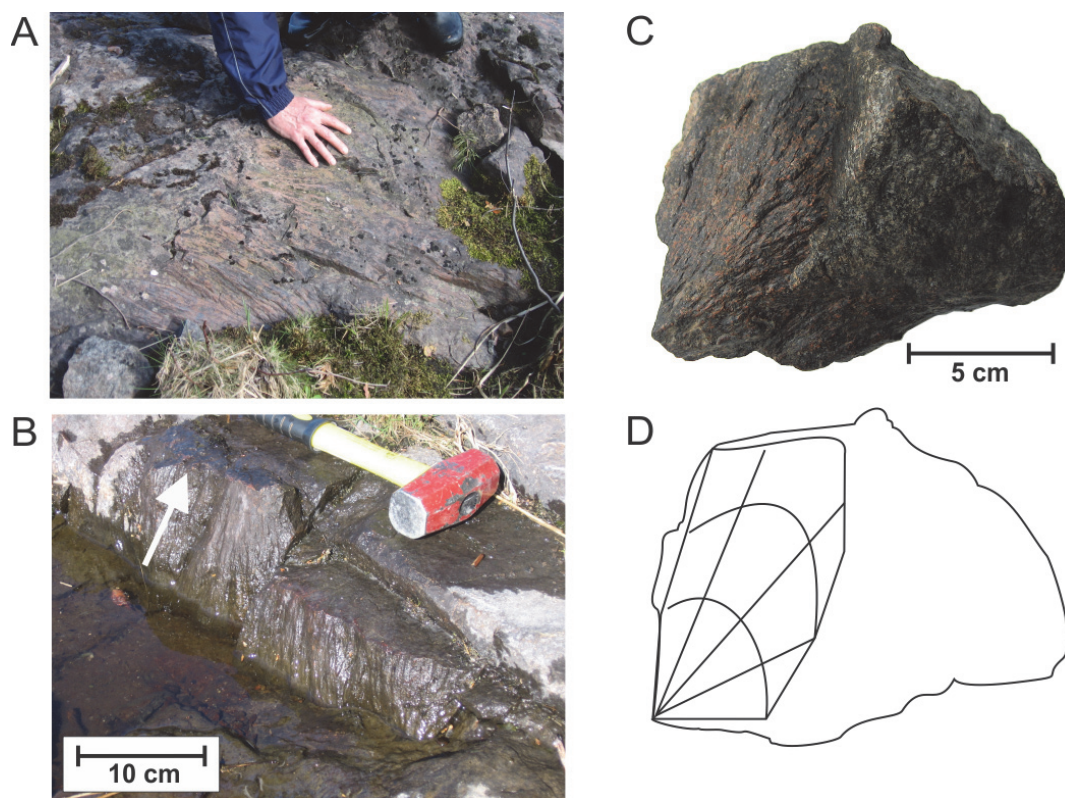

Fig. 2 (A) Glacial striations and their direction in bedrock shown by Martti Lehtinen, (B) vertical in-situ shatter cones (arrow shows the apex direction), (C) shatter cone boulder and (D) a line-drawing show the pointing apex.

2   *Geological background*

Keurusselkä structure is located within the Central Finland Granitoid Complex (CFGC) in the Svecofennian domain, which represents an accretionary orogenic belt formed at ca. 1900–1860 Ma (*Kähkönen,* 2005). The CFGC forms a major part of the Svecofennian upper continental crust containing both volcanic belts and large plutonic intrusions. In the Keurusselkä area, the granitoids, gneisses, gabbros and metavolcanic rocks form the characteristic lithology (*Nironen,* 2003) (Fig. 1). Other rock types are a

supracrustal schistoze zone situated in between granodioritic rocks and a Paleoprotero-zoic (1880 Ma) diabase dykes (*Puranen et al.,* 1992).

Three shallow drill holes (V-001, V-002 and V-003) drilled by Suomen Malmi Oy are located in the vicinity of the central uplift area (Fig. 1). The cores, described by *Raiskila et al.* (2012), consist of mica schists (metagraywackes), gneisses and felsic metavolcanic rocks. Core V-002 penetrates a 10-m-thick vein of monomictic breccia, which revealed possible impact glass altered into clay (chlorite, illite and smectite-group minerals) (*Raiskila et al.,* 2012). Preliminary geochemical analysis of breccia was done in order to solve the origin of altered glass (Dr. Johanna Salminen pers. comm. 2012), but further analyses to investigate possible meteoritic compounds in the clay minerals are in progress.

Impact-related lithologies, like impact melt or allochthonous breccias, have not been found in the Keurusselkä region. As the Keurusselkä structure is very old, the re-mains of these lithologies are likely absent in the nearby glacial till formations deposit-ed by the latest Fennoscandian ice ages. Even so, the probability to find the distal ejecta in the sedimentary sections of Baltica (Fennoscandia) or nearby locating Rodinia-continents (such as 1170 Ma Stoer group sediments in Scotland) remains a reality (*Amor et al.,* 2008*; Parnell et al.,* 2011). The temporal and compositional overlap be-tween the anorogenic and orogenic magmatism in west Baltica (East European craton) and east Laurentia (North America and Greenland), together with the paleomagnetic da-ta available from these two cratons, suggest that these continents coexisted for more than 600 Ma (from 1.8 to ~1.2 Ga), constituting the juxtaposition named NENA (North-ern Europe – North America; *Gower et al.,* 1990*; Salminen et al., in prep.*). By present standards, a rather limited paleomagnetic dataset support a NENA-like Mesoproterozoic reconstruction (*Patchett et al.,* 1978*; Piper,* 1980*; Buchan et al.,* 1990*; Pesonen et al.,* 2003). More recent data have appeared to support, within the analytical uncertainties, a single, long-lasting NENA juxtaposition between Baltica and Laurentia between ca. 1750 Ma and ca. 1270 Ma (*Salminen and Pesonen,* 2007*; Evans and Pisarevsky,* 2008*; Pisarevsky and Bylund,* 2010*; Pesonen et al.,* 2012), and perhaps enduring as long as ~1120 Ma (*Salminen et al.,* 2009) forming the core of Nuna together with Siberia (e.g. *Salminen and Pesonen,* 2007*; Wingate et al.,* 2009*; Lubnina et al.,* 2010*; Evans and Mitchell,* 2011) and possibly Amazonia (*Bispo-Santos et al.,* 2008*; Johansson* 2009). This compact Nuna configuration does not require identification of an additional craton to fill a 1000 km gap in previous reconstructions presented e.g. *Pisarevsky et al.* (2008) (*Evans and Mitchell,* 2011). Even though the Stoer group sediments are somewhat older (1170 Ma) compared to the age estimates for Keurusselkä structure (~1120 and 1140 Ma) (*Raiskila et al.,* 2011*; Schmieder et al.,* 2009), the fact that such Mesoproterozoic ejecta sections even exist, gives a change to link them to impact craters. We note that there is not yet found an impact crater, other than Keurusselkä, within a suitable age and size to match with the Stoer group ejecta (Earth Impact Database). Alternative known craters within Mesoproterozoic age are Suvasvesi N (age <1000 Ma, diameter 4 km), Lumparn (age ~1000 Ma, diameter ~9 km), Iso-Naakkima (age >1000 Ma, diameter ~3 km) and Santa Fe, New Mexico (age <1200 Ma, diameter ~6–13 km), although the lat-

ter is originally situated too far in NENA configuration to be linked with the Stoer group.

Lack of stratigraphic impact lithology suggests that the present erosion level of the Keurusselkä impact structure represents the sections between the crater floor and the transient crater floor (Fig. 4A). Along the approximate transient floor of the final crater, shock pressures may exceed 25–30 GPa at the center of the impact (*French,* 1998). The pressures drop rapidly (~25 GPa/few kilometers) down from the center of the impact (*Stöffler et al.,* 1988). At the crater rim pressures decrease to ≤2 GPa, which is minimum that is needed for the projectile to excavate into the target. Therefore, the present crosscut of the exposed crystalline basement of Keurusselkä structure with metamorphic shock features (PDFs) and 2–20 GPa pressures represents the sections between the crater floor and transient crater floor.

3   Geophysical features

3.1   Petrophysical and rock magnetic properties

Petrophysical and rock magnetic properties of samples collected from inside and outside the Keurusselkä structure were reported earlier (*Raiskila et al.,* 2011). The mean values are given in Table 1. Compared to density (2694±142 kgm^{-3}) of the metavolcanic rocks without shatter cones, the average densities (2578±273 kgm^{-3}) of metavolcanic rocks in the central parts of the structure are less. Relatively low densities (2532±187 kgm^{-3}) are characteristic for monomictic breccia from the drill core V-002. However, no such difference exists between the densities of granitic rocks with (granite 2728±87 kgm^{-3}) and without (granite 2703±151 kgm^{-3}, granodiorite 2715±99 kgm^{-3}) shatter cones.

Pesonen et al. (1999) have presented similar to the above-described densities from nearby located well-preserved Karikkoselkä structure (age 230–560 Ma, diameter 2.4 km; Fig. 1): impact breccia (2490 kgm^{-3}), fractured porphyry granite (2583–2691 kgm^{-3}) and unfractured granite (2603–2702 kgm^{-3}). Thus, the densities of the impact damaged crystalline target rocks are lower compared to the unshocked rocks.

Magnetic susceptibilities of the Keurusselkä granite are 365±245×10^6 SI and 1925±1895×10^6 SI for the rocks with and without shatter cones, respectively (Table 1). In contrast, felsic metavolcanic rocks with distinct shatter cones have higher susceptibilities (26,615±26,535×10^6 SI) compared to the metavolcanites without shatter coning (315±185×10^6 SI). Increased amounts of various sized magnetite in shatter cone bearing metavolcanic rocks was noticed to be the cause for the higher magnetizations (*Raiskila et al.,* 2011). Physical properties from schists (metagraywackes), gneisses and felsic metavolcanic rocks of the three drill cores in the vicinity of the Keurusselkä structure show susceptibilities similar to the granitic rocks without shatter coning. However, the core V-002 shows less variation in susceptibility than rocks from other cores; and the monomictic breccia vein shows petrophysical properties (Table 1) featuring the damaged crater basement (*Raiskila et al.,* 2012).

Table 1. Mean petrophysical properties of the Keurusselkä impact and target rocks (*Raiskila et al., 2011, 2012*).

Lithology	N(p)(n)	d (kgm^{-3})	k (10^{-6}SI)	J (mAm^{-1})	Q	P (%)	D_{NRM} (°)	I_{NRM} (°)
Target rocks without shatter cones								
Gabbro	18(9)(9)	3113±81	44,895±43,415	2733±2716	1.1±0.9	0.4±0.2	156	39
Tonalite	5(2)(2)	2607±25	6010±4600	44±31	0.2±0.1	1.1±0.2	23	67
Granite	122(7)(40)	2703±151	1925±1895	778±777	81±81	0.9±0.4	185	50
Granodiorite	53(2)(18)	2715±99	345±305	71±70	3.2±3.1	1.1±0.04	201	37
Porfyritic granodiorite	50(5)(17)	2783±130	425±345	33±31	4.8±4.7	0.8±0.4	315	48
Felsic metavolcanic rock	21(0)(6)	2694±142	365±245	5±4	0.3±0.2	-	223	58
Target rocks with shatter cones								
Granite	32(9)(14)	2728±87	315±185	23±21	2.7±2.6	0.7±0.1	183	58
Felsic metavolcanic rock	199(39)(67)	2578±273	26,615±26,535	718±717	4.3±4.3	0.9±0.6	173	60
Vilppula drill cores								
V-001 (Metagraywacke, -granodiorite, -volcanic rock)	37	2754±107	1505±1355	1159±1155	29±29	-	-	-
V-002 (Metagraywacke, -granodiorite, -volcanic rock)	30	2668±128	440±280	158±158	5.6±5.6	-	-	-
Monomictic breccia	12	2532±187	310±120	18.5±18.5	1,1±1.1	-	-	-
V-003 (Metagraywacke)	17	2774±116	1110±810	277±276	3.6±3.6	-	-	-

Notes: Statistical calculations were made using specimen level; N(p)(n), N= number of specimens used for calculating average values for petrophysics, p= number of specimens used for measuring porosity and nrm=number of specimens used for calculating declination and inclination of the remanent magnetization; d = density; k =magnetic susceptibility; J = intensity of natural remanent magnetization; Q = the Koenigsberger's ratio calculated for a field of 50 µT; P = porosity; D_{NRM} = declination of the natural remanent magnetization; I_{NRM} = inclination of the natural remanent magnetization.

3.2   Gravity data

Finnish Geodetic Institute (FGI) densified the national gravity network (average station distance 5 km) (*Kiviniemi,* 1980*; Kääriäinen and Mäkinen,* 1996) of the Keu-

russelkä area in summer 2005 by relative gravimetry campaign (gravimeter Scintrex CG5 and Geotrim's VRS-GPS network, Leica SR 530 GPS receiver and digital geoid model by FGI for height and positioning) in order to specify the gravity signature related to the structure (*Ruotsalainen et al.,* 2006). The pre-existing sparse national gravity network showed already some local Bouguer anomaly minimum in the area. Gravity densification profiles were measured approximately along the four cardinals and sub-cardinal points of compass from the anomaly minimum. Gravity measurements in Keuruselkä lake area were carried out on the islands instead of on the lake ice to avoid measurement uncertainties. Also, the Bouguer gravity reduction of water is unreliable, because of unknown bathymetry. Gravity influence of the Keuruselkä lake water mass was reduced from the observations by excluding gravity attraction of lake water with 6.4 m mean depth. Maximum reduction was as low as 0.064 mGal.

Local ~9 mGal Bouguer anomaly, corresponding to the granite intrusion between metavolcanic rocks in the central uplift area of Keurusselkä structure, was estimated by adjusting a plane to small local Bouguer anomaly maxima, which located 5–10 km from the minimum. This way the tilt of regional Bouguer anomaly was reduced to strengthen the local Bouguer anomaly features (Fig. 3A). Local Bouguer anomaly deviates only slightly from the original Bouguer anomaly and reduction of plane adjustment is only cosmetic. The overall circular gravity anomaly related to the impact structure is shown in Fig. 3A. More dense gravity station network (2 stations per 1 km^2) is, however, needed to improve the anomalous features.

Other smaller circular negative Bouguer anomalies in the region are mainly caused by younger (1860 Ma) granitic intrusions, which are recognized also in the geological map by *Nironen* (2003) and in aeromagnetic map as low amplitude regions (Fig. 3B).

3.3   *Aeromagnetic data*

The whole Keuruu area is covered with an aeromagnetic survey, with flight altitude of 30 and line spacing of 200 m. It was measured in 2007 by Geological Survey of Finland as a part of the national airborne geophysical mapping programme (*Hautaniemi et al.,* 2005). A high-amplitude (up to 500 nT) short-wavelength circular anomaly, ~6 km wide (Fig. 3B), is distinguished from the regional field. It partly coincides with the negative Bouguer anomaly, but does not extend as far to the east. Circular anomalies further away around the central magnetic high-amplitude anomaly are likely of regional origin or too complex to link to the impact structure.
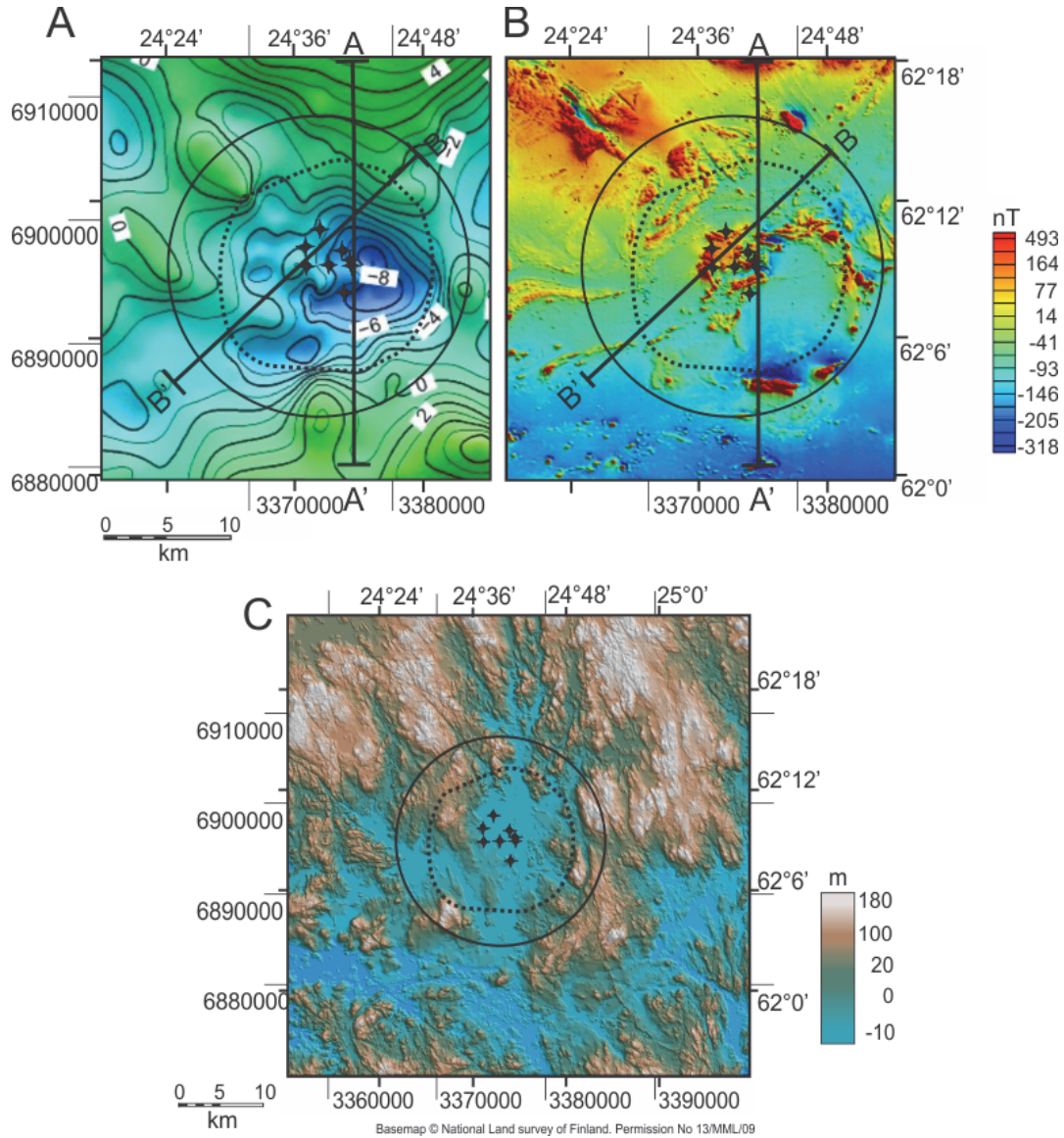
Fig. 3 (A) Local Bouguer gravity map (mean value of Bouguer gravity in the area reduced, values are in mGal) (courtesy of FGI), (B) Aeromagnetic map (courtesy of GTK) and (C) Digital elevation map (DEM) (courtesy of National Land Survey of Finland). Shatter cones are marked as black stars. The dotted circle indicates the area of damaged bedrock (D ~16 km). The solid circle marks the inner ring formation diameter (24.4 km) from Fig. 5.

3.4   Seismic profils

The FIRE2 profile (FIRE – The Finnish Reflection Experiment) (*Kukkonen and Lahtinen,* 2006) crosses eastern margin of the Keurusselkä structure (Fig. 1). The FIRE project provided crustal scale reflection seismic data of the deep structures (down to depths of 60 to 70 km) improving the knowledge of the evolution of the crust in the Finnish part of the Fennoscandian Shield. It produced seismic data with a broad frequency band and signal penetration of 20 s (two-way travel time) with a vertical resolution of few tens of meters. *Nironen et al.* (2006) presented a geological interpretation of the upper part of the crust. Furthermore, a tomographic analysis of the FIRE2 seismic

data was recently done to study the possible impact features (M. Malm, Institute of Seismology, University of Helsinki pers. comm. 2012). The velocity model of the seismic data did not show any clear boundaries that could be unambiguously tied with the Keurusselkä structure. However, within the structure area, lower seismic velocities were recognized from the depth range of 570 m (M. Malm pers. comm. 2012).

Seismic velocities of surface rock samples along the FIRE2 profile was measured by using instrumentation and methodology described by *Elbra et al.* (2011). Seismic velocities (Table 2) were obtained both in the laboratory (V_{P0} and V_{S0}; 0–1 MPa) and upper crustal pressure conditions (V_P and V_S; 100 MPa). The measured average V_{P0}, V_P and V_S values for the granite and granodiorite were 4386, 5373 and 2688 ms^{-1}. These, rather low seismic velocities for granitic rocks, indicate significant micro-fracturing. The measured low velocities do not, however, sufficiently correspond to the porosity values of selected samples presented in Table 1, which might indicate errors in porosity measurements done by using Archimedean method (*Kivekäs,* 1993).

Studies of seismic data from other meteorite impact structures have revealed indications of crater morphology (central uplift and crater rim). However, most of these investigations have concentrated on far less eroded marine structures (Chicxulub; *Morgan et al.,* 2000 and Mjølnir; *Tsikalas,* 2005, *Dypvik et al.,* 1996), structures buried by sediments (Chesapeake; *Poag et al.,* 1999 and Bosumtwi; *Scholz et al.,* 2002) or structures with sediment target lithology (Haughton; *Pohl et al.,* 1988*; Glass and Lee,* 2001).

Table 2. Seismic velocities obtained from rock specimens along FIRE2 seismic profile line in Fig. 1.

Lithology	Sample	V_{P0} (ms^{-1})	V_P (ms^{-1})	V_S (ms^{-1})	V_P/V_S
Porfyritic granodiorite	M-2	4160-4215	5351	2507	2.13
	M-3	4597	5313	2452	2.17
Granite	G-2	4467-4447	5611	2799	2.00
Granite	H-1	4586-4793	5426	2682	2.02
	H-5	4322-4664	5306	2897	1.83
Granite	K-4	3953-4402	5300	2755	1.92
	K-5	5091-5185	5707	3026	1.89
Granite	S-4	4651-4700	5461	2625	2.08
Gabbro	P-1	4071-4502	5314	2704	1.97
	P-4	3820-4117	4989	2286	2.18
Granite	O-2	4407-4423	5553	2645	2.10
	O-3	4066-4383	5147	2352	2.19
Granodiorite	N-3	4767	5677	2960	1.92

Note: V_{P0} is P-wave velocity in ambient pressure in laboratory conditions; V_P and V_S are P-wave and S-wave velocities in estimated crustal pressure conditions.

4   Crater dimensions

Scaling laws for dimensions of the crater structure (summarized e.g. by *Melosh,* 1989) were applied in order to investigate whether the theoretical values are in agreement with the observed anomalies over the Keurusselkä structure and if the calculations correspond to the models presented in this study.

A medium size impact crater (with rim-to-rim diameter $D \approx$ 4–50km) is of complex type with a central uplift (CU) (Fig. 4). Assuming the unambiguous shatter cones are located within the CU, and the approximate diameter of their coverage area D_{CU} is 6 km, original rim-to rim diameter D of a complex crater would be between 19.4 km ($D_{CU} = 0.31D$; *Therriault et al.,* 1997) and 27.3 km ($D_{CU} = 0.22D$; *Pike 1985*). The central structural uplift would be from 1.8 km to 2.6 km ($h_{CU} = 0.086D^{1.03}$; *Cintala and Grieve,* 1998) and the diameter of transient cavity D_{TC} from 12.8 to 24.7 km ($D_{TC} = D_Q^{0.15\pm0.04}\ D^{0.85\pm0.04}$, where $D_Q = 4$ km is the transition diameter from simple to complex structure; *Croft,* 1985). Most transient craters on Earth approach a parabolic shape for which transient crater depth h_{TC} is approximately 1/3 to 1/4 the diameter of transient cavity D_{TC} (*Melosh,* 1989). This would result to a transient crater depth of 3.2 km (rim-to-rim diameter 19.4 km) up to 8.2 km (rim-to-rim diameter 27.3 km).
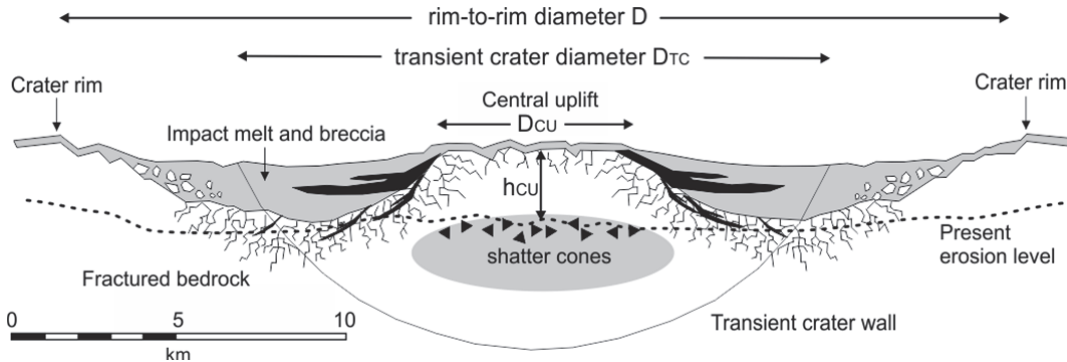

Fig. 4. Crosscut of a typical complex impact crater with central uplift (modified from *Melosh,* 1989 and *Abels,* 2003). Unevenly eroded erosion level suggested for Keurusselkä structure is marked with dashed line based on the field observations and the geophysical model.

To adapt these theoretical parameters to the Keurusselkä structure and its central uplift with shatter cones of a same size used in calculations above would imply a minimum crater diameter of 19.4–27.3 km, although the diameter of central uplift increases with erosion.

Digital elevation model (DEM) over the Keurusselkä region (Fig. 3C) shows that the eroded bedrock is partly covered with Quaternary deposits, which makes it difficult to identify the crater rim. The method of least squares was applied to the Bouguer gravity data. The results suggest three large circular features (Fig. 5) around the Keurusselkä structure. These features that run along maximum gravity peaks have diameters of 24.4 km, 75.6 km and 101 km. Focuses of the fitted rings point towards the center of Keurusselkä. The smallest ring (D = 24.4 km) matches well with the theoretical dimensions

of a rim-to-rim diameter calculated above using the diameter of an area with shatter cones ($D_{CU} \approx 6\ km$).
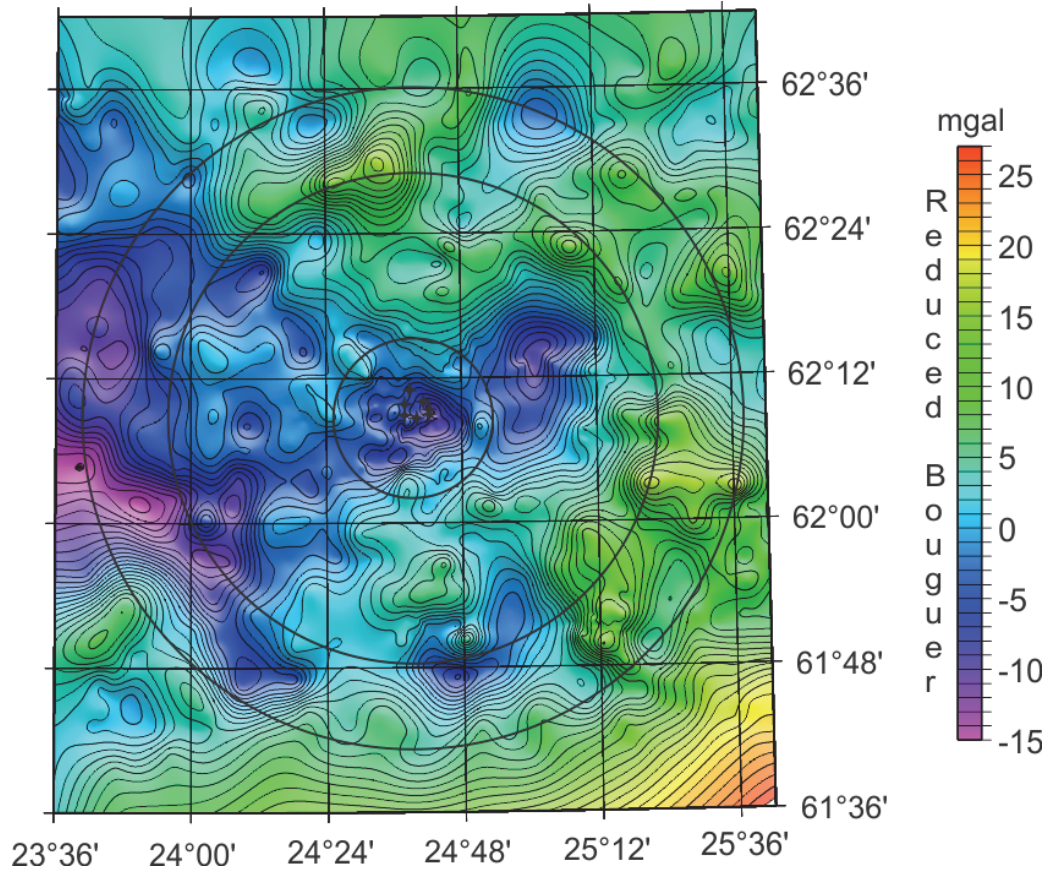

Fig. 5. Reduced Bouguer gravity map shows formation structures around the central uplift. Rings are calculated and fitted to the data using Least Square-method. The center of ring formations points to the center of the shatter cones. The inner formation has a diameter of 24.4 km. The middle and the outer formations have diameters of 75.6 km and 101 km.

5   *Gravity and magnetic models*

A joint (gravity and magnetic) 2.5-dimensional potential field modeling was carried out with Encom's ModelVision software along two profiles by using polygonal source bodies of target rocks and impact-influenced anomalous sources. Each modeled body has petrophysical properties (density and magnetization; Table 3) based on data from block (*Raiskila et al.,* 2011) and drill core (*Raiskila et al.,* 2012) samples (Table 1). The models (Figs. 6 and 7) describe a 2000 m deep section of the upper crust. The source body dimensions were adjusted to coincide with the calculated anomaly and the observed anomaly. The background density value used in the models is 2720 kgm^{-3} referring to the average crustal density of 2650–2800 kgm^{-3} (*Kuusisto et al.,* 2006). The local geomagnetic field intensity of 52123 nT, declination of 8° and inclination of 74° were used for the determination of induced magnetization of the source bodies. A background magnetic susceptibility was set to 500×10^{-6} SI.

Table 3. Petrophysical and dimensional properties of the model source bodies.

No.	Note	Lithology	Strike length (m)	d (kgm^{-3})	k (10^{-6}SI)	J (mAm^{-1})	Q	D$_{NRM}$ (°)	I$_{NRM}$ (°)
	Impact								
1	magnetized	Felsic metavolcanic rock	100	2500	26000	718	6.7	173	60
2	crater basement	Felsic metavolcanic rock	5000	2500	365	5	3.3	223	58
3	damaged	Felsic metavolcanic rock	5000	2570	365	5	3.3	223	58
4	damaged	Granite	5000	2570	315	2	1.5	183	58
	Bedrock								
	background	granitic		2720	500				
5		Gabbro	100	3000	45000	200	1.1	156	38
6		Tonalite	10000	2650	40000	200	1.2	22	66
7		granitic	10000	2800	500	5	2.5	200	50
8		granitic	10000	2740	1000	5	1.2	201	37
9		granitic		2700	1000	5	1.2	200	50
10	Hirsilä belt	Mica gneisses and schists		2780	1000	60	14	200	50

The profile A-A' (Fig. 6) next to the FIRE2 seismic profile line cuts the eastern margin of the circular central magnetic anomaly. The measured magnetic signal of the impact area shows a modest anomaly peak. The model is based on separate bodies: magnetized upper section (body 1), crater basement (body 2) and damaged granitic bedrock (body 4). The Keurusselkä impact area covers a bowl shape structure with a maximum depth of 1200 m of low density (2500–2550 kgm^{-3}). This area (D≈16 km) is marked in Fig. 1 with a dotted line. Densities of the source bodies agree with the measured surface densities (Table 1) and the low seismic velocities of the upper crust (Table 2).

The overall magnetic signal of the impact area is interfered by a gabbro intrusion (body 5). Even there is a density contrast between the background and gabbro, the intrusion is too small to produce an observable gravity signal. In the northern part of the profile A-A´, a tonalite intrusion (body 6) is responsible for a local magnetic high. The granitic bodies (7) below tonalite have typical granite/granodiorite values (Table 2). A small magnetic peak next to tonalite (at the distance of ~10000 m) indicates the possible continuation of the Keuruu diabase dykes or a nearby gabbro intrusion. The two peaks (~12000 m) show the boundary between granite and granodiorite. The boundary (~40000 m) between the CFGC granite and mica schist belt is also seen in aeromagnetic profile data.
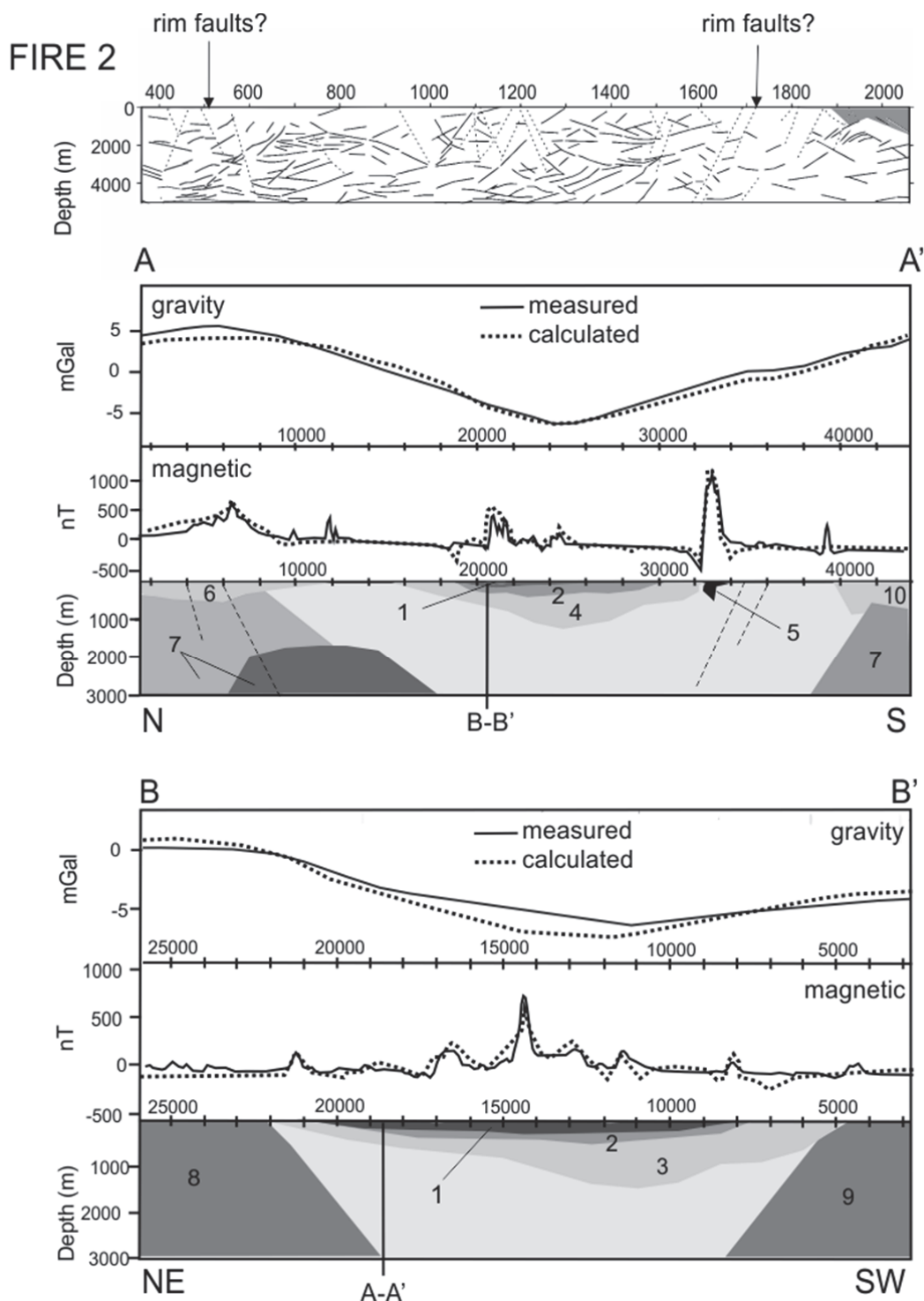
Fig. 6. Line drawing interpretation of the FIRE2 seismic profile shows a synform structure (*Nironen et al.,* 2006*)*. Possible rim faults have a diameter of ~24 km. Dark grey area on the right represents the gneissose schists (see Fig. 1). Combined gravity and aeromagnetic sections of model A-A' (NS) and model B-B' (SW-NE) over Keurusselkä impact structure show the damaged crater basement down to depth of 1200 m. Vertical lines B-B' and A-A' mark the cutting point of the two profiles.

The profile B-B' (Fig. 6) runs along the metavolcanic intrusion, crosses the circular magnetic anomaly (Fig. 3B) in the center of the Keurusselkä structure and the location of shallow drilling sites. The magnetic signal along the profile shows a striking central magnetic anomaly of a Sombrero-type shape, which is modeled with a layered construction of magnetized upper section (body 1), crater basement (body 2) and damaged felsic metavolcanic rock (body 3) beneath the structure, reaching a depth of 1200 m. The calculated Sombrero-type magnetic signal is achieved by shaping the height of the upper surface (0 to 20 m) of the magnetic source body according to DEM map (Fig. 5). However, the gravity signal is less varying in profile B-B' and do not require as deep damaged bedrock layers as profile A-A'. This might be due to similar lithology (metavolcanites), which do not have as strong contrasts as rocks in profile A-A'.

6   Discussion

Combining geophysical techniques and scaling laws, buried or eroded impact structures and their morphometric parameters can be revealed as based on geophysical potential field data. When dealing with deeply eroded structures, the geophysical anomalies could be the only source to estimate the crater dimensions. Majority of impact structures are characterized by potential field anomalies, such as circular gravity low and magnetic low or high caused by impact rocks and/or sediments covering the structure (*Pilkington and Grieve,* 1992*; Plado et al.,* 1999*; Henkel et al.,* 2002). The anomalies depend on the erosion level and the deformation degree of the impact structures. Erosion has an effect to the gravity anomalies by decreasing mostly the amplitudes, but not so much of the wavelength of the anomalies. In contrast, magnetic anomalies may change drastically during geological evolution as their source lithology is usually located within the allochthonous breccias and impact melts (*Plado et al.,* 1999).

Impacts on crystalline targets produce distinct changes in petrophysical properties causing contrasts between shocked and un-shocked target rocks. Generally, the density decreases due to impact generated fracturing and damage to the target. Therefore, the gravity signatures over simple and complex structures are an overall broad negative anomaly with possible gravity maximums of impact melt (e.g. Lappajärvi, *Elo et al.,* 1992) and/or central uplift. Keurusselkä is deeply eroded, meaning that the rim and the impact rock units have almost completely removed and only the magnetized and fractured crater basement is exposed. Yet, weak partly asymmetric morphological features can be seen around the central uplift (Fig. 3). Reasons for possible uneven erosion could be an oblique impact, geological anisotropy, or post-impact tectonic tilting. Good examples of morphological asymmetry are ~39 Ma old Haughton impact structure in Canada (D=23 km) (*Pohl et al.,* 1988*; Glass and Lee,* 2001) and ~142 Ma old marine impact structure Mjølnir in Barents Sea (D=40 km) (*Tsikalas,* 2005).

Collins et al. (2004) introduced a numerical model for a medium-sized crater and the typical deformational response of a granitic target to an impact event. They suggested that the strain model, where stresses, strains, and strain rates are all highest near the impact site and decrease with radial distance, should correlate with observed variations

in bulk density and seismic velocity. Especially, the seismic velocities obtained from specimens sampled along the FIRE2 seismic profile line show low velocities in granitic rocks indicating micro-fractured crater basement of damaged transient crater bedrock. Densities measured over Keurusselkä structure show decreased values particularly in felsic metavolcanic rocks with shatter cones ($D=2578\pm273\ kgm^{-3}$). To meet the measured gravity signal along the profiles the geophysical model (A-A' and B-B') requires a ~1200 m deep bowl structure ($D=2500–2550\ kgm^{-3}$). A consistent bowl shaped region, down to the depth of 1200 m, can also be identified from the line interpretation of FIRE 2 seismic profile data (*Nironen et al.,* 2006) (Fig. 6). *Nironen et al.* (2006) suggested for the seismic reflections either a possible synform structure of the Keurusselkä impact or granite outcropping at the surface. Our model (A-A' and B-B') highlights synform structures of less dense and fractured bedrock in Keurusselkä. The damaged area has a diameter of ~16 km and it explains the observed circular 6 mGal negative local Bouguer anomaly around the central uplift (Fig. 6). As the lake Keurusselkä is fairly shallow, the anomaly is linked to the less dense bedrock with low seismic velocities. The gravity data in the central parts of the structure is, however, asymmetric suggesting that the eastern part of the crater might have collapsed (profile A-A') (Fig. 3A). Other reasons could be unevenly crushed crater basement (A-A') or uplifted center (profile B-B'). In contrast to the Lappajärvi impact structure (age 73 Ma, diameter ~23 km), which has -11 mGal gravity anomaly, Keurusselkä could represent a ~0.5–1 km deeper section of the bedrock than Lappajärvi, based on the erosion estimation introduced by *Plado et al.* (1999).

Impact increases (or decreases) magnetizations of the target rocks and causes variations to the magnetic field. The magnetic signature over impact structures can be primarily the aggregate of: (1) composition and properties of target rocks, (2) modification of magnetic material in high P-T conditions and (3) natural remanent magnetization (NRM) (*Ugalde et al.,* 2005). The magnetic pattern of an impact structure is much more complicated and can differ remarkably from gravity anomaly showing either a broad magnetic low (*Sturkell and Ormö,* 1998) or a circular magnetic high (*Henkel et al.,* 2002). If central uplift takes place, it can produce a high-amplitude anomaly related to the uplifted rocks or impact melt. High pressures (~30 GPa) in the center of the structure induce shock remanent magnetization (SRM), which shows as a high amplitude and short wavelength magnetic anomaly (*Pilkington and Grieve,* 1992). Generally the magnetic anomalies in impact structures are related to melt and brecciation, but the crater floor can also exhibit enhanced magnetization produced by e.g. uplifted rock units or differentiated melt layers (*Ugalde et al.,* 2005).

The measured magnetic anomalies of the Keurusselkä impact structure are complex. Impact-induced changes in the aeromagnetic anomaly pattern have typical impact features of a strong circular anomaly in the center of the structure and an annular magnetic ring around the center (Fig. 3B and Fig. 6; profile B-B'), which is irregular due to geological heterogeneities and partly missing in the west of the Keurusselkä structure. The center magnetic anomalies are clearly related to the area with in-situ shatter cones with increased magnetizations, while the outer margin of the high-amplitude magnetic

anomaly in the central uplift is shown in profile A-A' (Fig. 6). The modification of magnetic minerals in high P-T conditions is likely the explanation to the observed high amplitude anomaly as rock material with in-situ shatter cones is more abundant with magnetite.

Interestingly, the nearby Lappajärvi impact structure (D = 23 km) does not have a clear magnetic central uplift anomaly. Compared to other structures, the magnetic anomalies of Keurusselkä structure are more similar to the Siljan impact structure (D = 52 km). In an aeromagnetic map of Siljan region by *Henkel and Aaro* (2005), a centrally located anomaly with positive amplitude of 500 nT and a diameter of 10 km is seen. These similarities suggest that the deeply eroded Keurusselkä structure has a corresponding size with the Siljan structure rather than with Lappajärvi structure. The reduced Bouguer anomaly of Keurusselkä region (Fig. 5) shows ring formations around Keurusselkä structure suggesting a larger size, but more evidence is needed to support this.

7   Conclusions

The aim of this study was to investigate the geophysical anomalies encountered in the Keurusselkä impact region and their depth dependence in the upper crust. Main interest was to estimate the original rim-to-rim diameter for the structure. Geophysical models based on petrophysical properties of rocks (and occurrence of shatter cones) provide information on causes of the geophysical anomalies related to the Keurusselkä impact structure. The high-amplitude magnetic anomaly in the center of the structure has a circular shape of an expanding ring wave, which is related to the magnetization of shatter cones. The increased magnetization in the central uplift area displays the effect of an impact into magnetic properties of the crystalline target rock. Observed gravity anomalies in Keurusselkä emphasize a bowl shaped area of fractured and damaged crater basement. Geophysical model revealed that changes in physical properties of rocks reach a depth of ~1200 m in an area with a diameter of ~16 km, which may represent the transient crater wall-to-wall diameter. Furthermore, the calculated theoretical parameters based on the diameter of the eroded central uplift, suggest diameter at least 19.4 km and up to 27.3 km. Geophysical features of Keurusselkä are not similar with the nearby Lappajärvi structure (diameter 23 km), but rather resemble with the Siljan structure (diameter 52 km) in Sweden. Therefore, based on the aspects presented here and the obtained geophysical models, we propose that the original rim-to-rim diameter of Keurusselkä structure has been at least 24–27 km.

References

Abels, A., 2003. Investigation of impact structures in Finland (Söderfjärden, Lappajärvi, Lumparn) by digital integration of multidisciplinary geodata. PhD thesis, Westphalian-Wilhelms University Münster, Germany.

Amor, K., S.P. Hesselbo, D. Porcelli, S. Thackery and J. Parnell, 2008. A Precambrian proximal ejecta blanket from Scotland. *Geology* **36**, 303–306.

Baratoux, D. and H.J. Melosh, 2003. The formation of shatter cones by shock wave interference during impacting. *Earth and Planetary Science letters* **216**(1–2), 43–54.

Bispo-Santos, F., M. D'Agrella-Filho, I. Pacca, L. Janikian, R. Trindale, S.-Å. Elming, J. Silva, M. Barros and F. Pinho, 2008. Columbia revisited: Paleomagnetic results from the 1790 Ma collider volcanics (SW Amazonian Craton, Brazil). *Precambrian Research* **164**(1–2), 40–49.

Buchan, K.L. and H.C. Halls, 1990. Paleomagnetism of Proterozoicmafic dyke swarms of the Canadian Shield. In: Parker, A.J., Rickwood, P.C., Tucker, D.H. (Eds.), *Mafic Dykes and Emplacement Mechanisms*. Balkema, Rotterdam, 209–230.

Cintala, M.J. and R.A.F. Grieve, 1998. Scaling impact melting and crater dimensions: Implications for the lunar cratering record. *Meteoritics & Planetary Science* **33**, 889–912.

Collins, G.S., H.J. Melosh and B.A. Ivanov, 2004. Modeling damage and deformation in impact simulations. *Meteoritics & Planetary Science* **39**(2), 217–231.

Croft, S.K., 1985. The scaling of complex craters. *Proceedings Lunar and Planetary Science Conference 15, Part 2; Journal of Geophysical Research* **90** (Supplement), C828–C842.

Dypvik, H., J. Plado, C. Heinberg, E. Håkansson, L.J. Pesonen and S. Raiskila, 2008. Impact structures and events – a Nordic perspective. *Episodes* **31**(1), 107–114.

Dypvik, H., S.T. Gudlaugsson, F. Tsikalas, M. Jr. Attrep, R.E. Jr. Ferrell, D.H. Krinsley, A. Mork, J.I. Faleide and J. Nagy, 1996. Mjølnir structure: An impact crater in the Barents Sea. *Geology* **24**, 779–782.

Elbra, T., R. Karlqvist, I. Lassila, E. Haeggström and L.J. Pesonen, 2011. Laboratory measurements of the seismic velocities and other petrophysical properties of the Outokumpu deep drill core samples, eastern Finland. *Geophysical Journal International* **184**(1), 405–415.

Elo, S., T. Jokinen and H. Soininen, 1992. Geophysical investigations of the Lake Lappajärvi impact structure, western Finland. *Tectonophysics* **216,** 99–109.

Evans, D.A.D. and R.N. Mitchell, 2011. Assembly and breakup of the core of Paleo-Mesoproterozoic supercontinent Nuna. *Geology* **39,** 443–446.

Evans, D.A.D. and S.A. Pisarevsky, 2008. Plate tectonics on early Earth? -weighing the paleomagnetic evidence. In: Condie, K. & Pease, V., eds., When Did Plate Tectonics Begin? *Geological Society of America Special Paper* **440**, 249–263.

Ferrière, L. S. Raiskila, G.R. Osinski, L.J. Pesonen and M. Lehtinen, 2010. The Keurusselkä impact structure, Finland – Impact origin confirmed by characterization of planar deformation features in quartz grains. *Meteoritics & Planetary Science* **45**(3), 434–446.

French, B.M. and C. Koeberl, 2010. The convincing identificaton of terrestrial meteorite impact structures: What works, what doesn't, and why. *Earth Science Reviews* **98**, 123–170.

French, B.M. 1998. Traces of Catastrophe: A handbook of shock-metamorphic effects in terrestrial meteorite impact structures. LPI Contribution 954. Houston, Texas: Lunar and Planetary Institute. 120 p.

Glass, B.J. and P. Lee, 2001. Airborne Geomagnetic Investigation at the Haughton Impact Structure, Devon Island, Nunavut, Canada. Lunar and Planetary Science XXXII, Abstract 2155.

Gower, C.F., A.F. Ryan and T. Rivers, 1990. Mid-Proterozoic Laurentia–Baltica: an overview of its geological evolution and a summary of the contributions made by this volume. In: Gower, C.F., Rivers, T., Ryan, B. (Eds.), *Mid Proterozoic Laurentia–Baltica*. Geological Association of Canada, St. John's Newfoundland, 23–40.

Hautaniemi H., Kurimo M., Multala J., Leväniemi H. and Vironmäki J., 2005. The "Three in One" aerogeophysical concept of GTK in 2004, In: Airo, M-L. (Ed.). *Aerogeophysics in Finland 1972–2004: Methods, System Characterizatics and applications*.Geological Survey of Finland Special Paper **39**, 21–74.

Henkel, H., W.U. Reimold and C. Koeberl, 2002. Magnetic and gravity model of the Morokweng impact structure. *Journal of Applied Geophysics* **49**, 129–147.

Henkel, H. and S. Aaro, 2005. Geophysical investigation of the Siljan Impact Structure – A short review. In: Koeberl C. and Henkel H. (Eds.) *Impact tactonics*. Springer, Berlin, 247–284.

Hietala, S. and J. Moilanen, 2004. Keurusselkä- A New Impact Structure in central Finland. *XXXV Lunar and Planetary Science Conference*, Abstract 1619.

Hietala, S. and J. Moilanen, 2007. Keurusselkä- Distribution of shatter cones. *XXXVIII Lunar and Planetary Science Conference*, Abstract 1762.

Johansson, A. 2009. Baltica, Amazonia and the SAMBA connection – 1000 milion years of neighbourhood during the Proterozoic? *Precambrian Research* **175**(1–4), 221–234.

Kivekäs, L. 1993. Density and porosity measurements at the petropysical laboratory of the Geological Survey of Finland. In: Autio S. (Ed.) *Geological Survey of Finland, current research 1991–1992.* Geological Survey of Finland Special Paper 18. Espoo, 119–127.

Kiviniemi, A., 1980. Gravity measurements in 1961–1978 and the results of the gravity survey of Finland in 1945–1978. *Publications of the Finnish Geodetic Institute*, **91**.

Kukkonen, I. and R. Laitinen, 2006. Finnish Reflection Experiment FIRE 2001–2005. Geological Survey of Finland, *Special Paper* **43**.

Kuusisto, M., I.T. Kukkonen, P. Heikkinen and L.J. Pesonen, 2006. Lithological interpretation of crustal composition in the Fennoscandian Shield with seismic velocity data. *Tectonophysics* **420**, 283–299.

Kähkönen, Y., 2005. Svecofennian supracrustual rocks, in: Lehtinen M., Nurmi P.A. and Rämö T. (Eds.), *Precambrian geology of Finland – Key to the evolution of the Fennoscandian shield*. Elsevier, Developments in Precambrian Geology, Amsterdam, 343–406.

Kääriäinen, J. and J. Mäkinen, 1997. The 1979–1996 gravity survey and results of the gravity survey of Finland. *Publications of the Finnish Geodetic Institute* **125**, 47–56.

Lubnina, N., S. Mertanen, U. Söderlund, S. Bogdanova, T. Vasilieva and D. Frank-Kramenetsky, 2010. A new key pole for the East European Craton at 1452 Ma: Palaeomagnetic and geochronological constraints from mafic rocks in the Lake Ladoga region (Russian Karelia). *Precambrian Research* **183**(3), 442–462.

Melosh, H.J., 1989. Impact Cratering: A Geologic Process. Oxford University Press, New York.

Morgan, J., M. Warner, G. Collins, H.J. Melosh and G. Christeson, 2000. Peak-ring formation in large impact craters: geophysical constraints from Chicxulub. *Earth and Planetary Science Letters* **183**(3–4), 347–354.

Nironen, M., 2003. Central Finland Granitoid Complex- Explanation to a map. *Report of Investigation* **157**. Geological Survey of Finland.

Nironen, M., A. Korja A., P. Heikkinen and the FIRE Working Group, 2006. A geological interpretation of the upper crust along FIRE2 and FIRE2A. In: Kukkonen I. and Laitinen R. (Eds.), *Finnish Reflection Experiment FIRE 2001–2005*. Geological Survey of Finland, Special Paper **43**, 77–104.

Parnell, J., M. Darren, A.E. Fallick, A. Boyce and S. Thackrey, 2011. The age of the Mesoproterozoic Stoer Group sedimentary and impact deposits, NW Scotland. *Journal of the Geological Society* **168**(2), 349–358.

Patchett, P.J., G. Bylund and B.G.J. Upton, 1978 Palaeomagnetism and the Grenville orogeny: New Rb-Sr ages from dolerites in Canada and Greenland. *Earth and Planetary Science Letters* **40**(3), 349–364.

Pesonen, L.J., S. Mertanen and T. Veikkolainen, 2012. Paleo-Mesoproterozoic Supercontinents – A Paleomagnetic view. *Geophysica* **48**(1–2), 5–47.

Pesonen, L.J., S.-Å. Elming, S. Mertanen, S. Pisarevsky, M. D'Agrella-Filho, J.G. Meert, P.W. Schmidt, N. Abrahamsen and G. Bylund, 2003. Palaeomagnetic configuration of continents during the Proterozoic. *Tectonophysics* **375**(1–4), 289–324.

Pesonen, L.J., S. Elo, M. Lehtinen, T. Jokinen, R. Puranen and L. Kivekäs, 1999. Lake Karikkoselkä impact structure, central Finland: New geophysical and petrographic results. GSA Special papers **339**, 131–147.

Pike, R.J. 1985. Some morphological systematics of complex impact structures. *Meteoritics,* **20**, 49–68.

Pilkington, M. and Grieve, R.A.F., 1992. The geophysical signature of terrestrial impact craters. *Reviews of Geophysics* **30**(2), 161–181.

Piper, J.D.A. 1980. A paleomagnetic study of Svecofennian basic rocks: Middle Proterozoic configuration of the Fennoscandian, Laurentian and Siberian shields, *Phys. Earth Planet. Int.*, **23**, 165 – 187.

Pisarevsky, S.A. and G. Bylund, 2010. Paleomagnetism of 1780–1770 Ma mafic and composite intrusions of Småland (Sweden): implications for the mesoproterozoic supercontinent. *American Journal of Science* **310**(9), 1168–1186.

Pisarevsky, S.A., L.M. Natapov, T.V. Donskaya, D.P. Gladkochub and V.A. Vernikovsky, 2008. Proterozoic Siberia: A promontory of Rodinia. *Precambrian Research* **160**(1–2), 66–76.

Plado, J., L.J. Pesonen and V. Puura, 1999. Effect of erosion on gravity and magnetic signatures of complex impact structures: Geophysical modeling and applications. In: Dressler, B.O., Sharpton, V.L. (Eds.) *Large Meteorite Impacts and Planetary Evolution II*. Geological Society of America, Special Paper **339**, 229–239.

Poag, C.W., D.R. Hutchinson, S.M. Colman and M.W. Lee, 1999. Seismic expression of the Chesapeake Bay impact crater: structural and morphologic refinements based on new seismic data. GSA Special Paper **339**, 149–164.

Pohl, J., A. Eckstalle and P.B. Robertson, 1988. Gravity and Magnetic Investigation of the Haughton Impact Structure, Devon Island, Canada. *Meteoritics* **23**, 235–238.

Puranen, R., L.J. Pekkarinen and L.J. Pesonen, 1992. Interpretation of magnetic fabrics in the early proterozoic diabase dykes of Keuruu, central Finland. *Physics of the Earth and Planetary Interiors* **72**(1), 68–82.

Raiskila, S., J. Salminen, T. Elbra and L.J. Pesonen, 2011. Rock magnetic and paleomagnetic study of the Keurusselkä impact structure, central Finland. *Meteoritics & Planetary Science* **46**(11), 1670–1687.

Raiskila, S., P. Heikkilä, U. Preeden and L.J. Pesonen, 2012. Physical properties of the Vilppula drill cores and petrographic analysis of associated breccias in Keurusselkä impact structure, central Finland. *Studia Geophysica et Geodaetica* **56**(2), 659–676.

Ruotsalainen, H., S. Hietala, M. Poutanen, J. Moilanen and L.J. Pesonen, 2006. Gravity survey of the Keurusselkä meteorite impact structure, central Finland. *Bulletin of the Geological Society of Finland, Special Issue* **1**, 134.

Salminen, J., L.J. Pesonen, S. Mertanen, J. Vuollo, and M.-L. Airo, 2009. Paleomagnetism of Salla Diabase Dyke, northeastern Finland and its implication to the Baltica-Laurentia entity during Mesoproterozoic. In: Reddy S. S., Mazumber R., and Evans D.A.D.(Eds.) *Paleoproterozoic supercontinents and global evolution*. London, Geological Society of London Publications **232**, 199–217.

Salminen, J. and L.J. Pesonen, 2007. Paleomagnetic and rock magnetic study of the Mesoproterozoic sill, Valaam Island, Russian Karelia. *Precambrian Research* **159**(3–4), 212–230.

Schmieder, M., F. Jourdan, S. Hietala, J. Moilanen, T. Öhman and E. Buchner, 2009. A high-precision Late Mesoproterozoic 40Ar/39Ar age for the Keurusseljä impact structure (Finland). *XXXX Lunar and Planetary Science Conference*, Abstract 1028.

Scholz, C., T. Karp, K. Brooks, B. Milkereit, P. Amoako and J. Arko, 2002. Pronounced central uplift identified in the Bosumtwi impact structure, Ghana, using multi-channel seismic reflection data. *Geology* **30**(10), 939–942.

Sturkell, E.F.F. and J. Ormö, 1998. Magnetometry of the marine, Ordovician Lockne impact structure, Jämtland, Sweden. *Journal of Applied Geophysics* **38**, 195–207.

Stöffler, D., L. Bischoff, W. Oskierski and B. Wiest, 1988. Structural deformation, breccia formation and shock metamorphism in the basement of complex terrestrial impact craters: Implications for the cratering process. In: Bodén A. and Eriksson K.G. (Eds.). *Deep drillings in crystalline bedrock 1*. Springer-Verlag, Berlin, 277–297.

Therriault, A.M., R.A.F. Grieve and W.U. Reimold, 1997, Original size of the Vredefort structure: Implications for the geological evolution of the Witwatersrand Basin. *Meteoritics & Planetary Science* **32**, 71–77.

Tsikalas, F., 2005. Mjølnir crater as a result of oblique impact: Asymmetry evidence constrains impact direction and angle. In: Koeberl C. and Henkel H. (Eds.) *Impact tectonics*. Springer-Verlag, Berlin, 285–306.

Ugalde, H.A., N. Artemieva and B. Milkereit, 2005. Magnetization on impact structures – Constraints from numerical modeling and petrophysics. In: Kenkmann T., Hörz F. and Deutch A. (Eds.) *Large meteorite impacts III*. Geological Society of America, 25–42.

Wieland, F., W.U. Reimold and R.L. Gibson, 2006. New observations of shatter cones in the Vredefort impact structure, South Africa, and evaluation of current hypotheses for shatter cone formation. *Meteoritics & Planetary Science* **41**(11), 1737–1759.

Wingate, M., S. Pisarevsky, D. Gladkochub, T. Donskaya, K. Konstantinov, A. Mazukabzov and A. Stanevich, 2009. Geochronology and paleomagnetism of mafic igneous rocks in the Olenek Uplift, northern Siberia: Implications for Mesoproterozoic supercontinents and paleogeography. *Precambrian Research* **170**(3–4), 256–266.